Mathematical Modelling of Groundwater Quality Measurement around a Landfill for Residential Water Usage

Nattawut Pongnu, and Nopparat Pochai

Abstract—**Leachate from a landfill has the potential to pollute groundwater. Mathematical models are often used to describe groundwater circulation, which can help planners choose suitable places for a landfill. The construction of landfills may have an influence on the groundwater supplies of adjacent settlements. As a result, impact assessments must be completed prior to the start of the project. This study used three mathematical models to simulate groundwater contamination concentrations with variable flow velocities. The first model is a groundwater flow model that estimates the hydraulic head of groundwater flow. The second model is used to calculate the groundwater flow velocity. The third model is a dispersion model, in which the governing factor is the two-dimensional dispersion equation, which yields the groundwater pollution concentration. In the simulation phase, we use the finite difference method for all models. This investigation considers the effects of industrial water usage, such as pumping water up to the surface, on groundwater flow. This research focuses on the effects of pumping water to adjacent settlements on groundwater flow and the quality of the water produced. Construction of a landfill should always be done in an area with a low hydraulic head. Pumping wells near landfills may also assist to reduce pollution in household groundwater. As a result, the calculated water quality in the faraway area was improved while groundwater volume and flow velocity were preserved.**

Index Terms—**hydraulic head, groundwater flow model, dispersion model, groundwater pollutant concentration**

I. Introduction

THE comparison each waste disposal methods, landfill is the simplest and cheapest way to deal with waste. It has been a popular method all over the world for hundreds of years. It was wrongly believed that there would be no problem with landfills due to the leakage of garbage juice from landfill sites into groundwater. Compacted soil was thought to be a great natural filter. A study discovered that landfill leakage had an effect on groundwater quality. To reduce the impact of leakage, landfill waste was separated into general solid waste and hazardous waste. Although a protection is placed under a landfill to protect the leakage to soil, there is still leakage occurring.

The finite difference [1, 2, 3] and finite element methods [4, 5, 6] are the most popular numerical solution techniques for groundwater flow models. A useful spreadsheet for two and three dimensional steady-state and transient groundwater numerical simulation in proposed in [7, 8]. The mathematical model [9] is used to simulate soil salinity in the area near marine shrimp aquaculture farm by using the electrical conductivity, an indicator of soil salinity assessment. A couple mathematical models of groundwater flow [10] are used to simulate the soil salinity in the area near marine shrimp aquaculture farm. The alternating direction methods are used to approximate the hydraulic head level of groundwater flow model [11]. In [12], the mathematical simulation of groundwater management in drought area is used to optimal management of the water injection stations to achieve minimum cost. A two-dimensional mathematical model [13] is proposed to investigate groundwater pollutant concentration around a land fill for long-term. In [14], a one-dimensional transient advection-diffusion equation is used to describe groundwater pollutant concentration measurement and to appoximate these equation by using the standard fourth-order finite difference methods with Saulyev Scheme and a modified fourth-order finite difference methods with Saulyev Scheme. The new fourth-order finite difference technique with Saulyev method [15] is used to approximate groundwater pollutant concentration in an area around a landfill. The numerical simulations of one-dimensional groundwater pollution measurement around landfills models through heterogeneous soil is represented by [16]. The mathematical models [17] is used to explain groundwater contamination with chloride and their substance. The two-level explicit method, the lax-wendroff method and the traditional upwind method [18] are used to approximate a better solution of groundwater quality assessment model.

In this research, three mathematical models are applied to simulate the groundwater pollution concentration with varied flow velocity. The first is the groundwater flow model, which provides the hydraulic head. The second is the flow velocity model, in which the hydraulic head is transformed into the velocity field of groundwater flow. The third is a dispersion model, in which the two-dimensional dispersion equation, which yields the groundwater pollutant concentration, is a regularly employed controlling factor. For three models, we apply the finite difference techniques in the simulation procedure. Finally, we offer a numerical simulation that validates the technique's results.

II. Mathematical Model

A. Groundwater Flow Model

We consider the governing equation of vertically integrated Darcy's flow in a two-dimensional confined, compressible,

Manuscript received December 15, 2021; revised May 22, 2022.

This paper is supported by Centre of Excellence in Mathematics, Ministry of Higher Education, Science, Research and Innovation Bangkok, Thailand.

Nattawut Pongnu is a Lecturer at Faculty of Sports Sience and Health, Thailand National Sports University Udon Thani Campus, Udon Thani 41000, Thailand. (e-mail: orange_np@hotmail.com.)

Nopparat Pochai is an Assistant Professor at Department of Mathematics, Faculty of Science, King Mongkut's Institute of Technology Ladkrabang, Bangkok 10520, Thailand. (Corresponding author to provide phone: 662-329-8400; fax: 662-329-8400; e-mail: nop_math@yahoo.com.)

isotropic, heterogeneous aquifer is [8],

$$S\frac{\partial H}{\partial t} = \frac{\partial}{\partial x}\left(K\frac{\partial H}{\partial x}\right) + \frac{\partial}{\partial y}\left(K\frac{\partial H}{\partial y}\right) \pm W, \tag{1}$$

where $H(x, y, t)$ is hydraulic head (metre), $K(x, y)$ is hydraulic conductivity (metre/day), $W(x, y)$ is sinks and/or source (1/day) and S is matrix of specific storage (1/metre). In this research, we assume the hydraulic conductivity is constant. It is obtain that

$$S\frac{\partial h}{\partial t} = K\left(\frac{\partial^2 H}{\partial x^2} + \frac{\partial^2 H}{\partial y^2}\right) \pm W. \tag{2}$$

The boundary conditions are specified for all $(x, y) \in [0, L] \times [0, M]$ where L and M are positive constants which represent the dimension of the rectangular domain, the initial conditions for $t = 0$ are specified,

$$H(x, y, 0) = H_Z(y) \tag{3}$$

at $x = 0$ and $0 \le y \le M$,

$$H(x, y, 0) = H_0(x, y) \tag{4}$$

at $0 < x \le L$ and $0 \le y \le M$.

The boundary condition for $t > 0$ are specified,

$$\frac{\partial H}{\partial n} = H_N \tag{5}$$

at $0 \le x \le L$ and $y = M$,

$$\frac{\partial H}{\partial n} = H_S \tag{6}$$

at $0 \le x \le L$ and $y = 0$,

$$H(x, y, t) = H_Z(y) \tag{7}$$

at $x = 0$ and $0 \le y \le M$,

$$\frac{\partial H}{\partial n} = H_E \tag{8}$$

at $x = L$ and $0 \le y \le M$, where H_N, H_S and H_E are known constants, H_Z and H_0 are known functions.

And the source terms $W(x, y)$ that represented by the rate of pumping well in each point,

$$W(x_s, y_s) = Q(x_s, y_s) = Q_s, \tag{9}$$

for all $s = 1, 2, 3, \cdots, p$, where s is number of pumping wells.

B. Flow Velocity Model

Darcy's law is an equation that describes a fluid's capacity to flow through a porous medium like rock. It is based on the idea that the quantity of flow between two places is directly proportional to the difference in pressure between the points and the media's capacity to obstruct the flow. Here pressure refers to the excess of local pressure over the normal hydrostatic fluid pressure which, due to gravity, increases with depth like in a standing column of water. Permeability is the term for the flow impedance factor. Darcy's law is a straightforward proportional connection between the instantaneous discharge rate through a porous medium and the pressure decrease over a certain distance. In modern format, using a particular sign convention, Darcy's law is usually written as

$$q = -K\frac{\partial H}{\partial L}, \tag{10}$$

where q is the velocity in L-direction, $K(x, y)$ is hydraulic conductivity (metre/day) and is hydraulic head (metre). This research rewrite equation (10) by

$$U = -K\frac{\partial H}{\partial x}, \tag{11}$$

$$V = -K\frac{\partial H}{\partial y}, \tag{12}$$

where $U(x, y, t)$ is the velocity in x-direction and $V(x, y, t)$ is velocity in y-direction.

C. Dispersion Model

Mass conservation of conservative solutes transported through media is described by a partial differential equation known as advection-dispersion. Measurement solute concentration around waste landfill, we consider the governing equation of the dynamic two-dimensional advection-dispersion equations as follow,

$$\frac{\partial C}{\partial t} = D_x\frac{\partial^2 C}{\partial x^2} + D_y\frac{\partial^2 C}{\partial y^2} - U\frac{\partial C}{\partial x} - V\frac{\partial C}{\partial y}, \tag{13}$$

where $C(x, y, t)$ is pollution concentration of groundwater, $U(x, y, t)$ is the velocity in x-direction and $V(x, y, t)$ is velocity in y-direction, D_x and D_y are diffusion coefficients of diffusion terms in the both directions on dispersion equation. The The boundary conditions are specified for all $(x, y) \in [0, L] \times [0, M]$ where L and M are positive constants which represent the dimension of the rectangular domain, the initial conditions for $t = 0$ are specified,

$$C(x, y, 0) = C_Z(y) \tag{14}$$

at $x = 0$ and $0 \le y \le M$,

$$C(x, y, 0) = C_0(x, y) \tag{15}$$

at $0 < x \le L$ and $0 \le y \le M$.

The boundary condition for $t > 0$ are specified,

$$\frac{\partial C}{\partial n} = C_N \tag{16}$$

at $0 \le x \le L$ and $y = M$,

$$\frac{\partial C}{\partial n} = C_S \tag{17}$$

at $0 \le x \le L$ and $y = 0$,

$$C(x, y, t) = C_Z(y) \tag{18}$$

at $x = 0$ and $0 \le y \le M$,

$$\frac{\partial C}{\partial n} = C_E \tag{19}$$

at $x = L$ and $0 \le y \le M$, where C_N, C_S and C_E are known constants, C_Z and C_0 are known functions.

III. Numerical Techniques

A. Finite Difference Method for the Groundwater Flow Model

We will propose the forward time central space method (FTCS) to the transient groundwater model. We discretize equation (2) by dividing the interval $[0, L]$ in x-direction into I subintervals such that $I\Delta x = L$, the interval $[0, M]$ in y-direction into J subintervals such that $J\Delta y = M$ and the interval $[0, T]$ in time into N subintervals such that $N\Delta t = T$. We can then approximate $H(x, y, t)$ by $H^n_{i,j}$, value of the difference approximation of $H(x, y, t)$ at point $x = i\Delta x$, $y = j\Delta y$ and $x = n\Delta t$ where $0 \leq i \leq I$, $0 \leq j \leq J$ and $0 \leq n \leq N$ which i, j and n are positive integers.

Taking the central difference scheme in space and forward difference scheme in time into each terms of equation (2), then

$$\frac{\partial^2 H}{\partial x^2} \approx \frac{H^n_{i-1,j} - 2H^n_{i,j} + H^n_{i+1,j}}{(\Delta x)^2}, \tag{20}$$

$$\frac{\partial^2 H}{\partial y^2} \approx \frac{H^n_{i,j-1} - 2H^n_{i,j} + H^n_{i,j+1}}{(\Delta y)^2}, \tag{21}$$

$$\frac{\partial H}{\partial t} \approx \frac{H^{n+1}_{i,j} - H^n_{i,j}}{\Delta t}, \tag{22}$$

$$W^n_{i,j} = \pm \frac{Q^n_{i,j}}{\Delta x \Delta y H^n_{i,j}}. \tag{23}$$

Substituting equation (20)-(23) into equation (2), for $1 < i < I - 1$ and $1 < j < J - 1$ at $t > 0$,

$$\begin{aligned} H^{n+1}_{i,j} &= H^n_{i,j} + \xi \left(H^n_{i+1,j} - 2H^n_{i,j} + H^n_{i-1,j} \right) \\ &+ \eta \left(H^n_{i,j+1} - 2H^n_{i,j} + H^n_{i,j-1} \right) + \omega \left(\frac{Q^n_{i,j}}{\Delta x \Delta y H^n_{i,j}} \right), \end{aligned} \tag{24}$$

where $\xi = \frac{(\Delta t)K}{(\Delta x)^2 S}$, $\eta = \frac{(\Delta t)K}{(\Delta y)^2 S}$ and $\omega = \frac{\Delta t}{S}$.

For $i = 1$ and $j = 1$ at $t > 0$, substituting the known values on west boundary by $H^n_{0,1} = H_1$ and substituting the unknown value on the south boundary by forward difference approximation $H^n_{1,0} = H^n_{1,1} - (\Delta y) H_S$,

$$\begin{aligned} H^{n+1}_{1,1} &= H^n_{1,1} + \xi \left(H^n_{2,1} - 2H^n_{1,1} + H_1 \right) \\ &+ \eta \left(H^n_{1,2} - H^n_{1,1} - (\Delta y) H_S \right) + \omega \left(\frac{Q^n_{1,1}}{\Delta x \Delta y H^n_{1,1}} \right). \end{aligned} \tag{25}$$

For $1 < i < I - 1$ and $j = 1$ at $t > 0$, substituting the unknown value on the south boundary by the forward difference approximation $H^n_{i,0} = H^n_{i,1} - (\Delta y) H_S$,

$$\begin{aligned} H^{n+1}_{i,j} &= H^n_{i,1} + \xi \left(H^n_{i+1,1} - 2H^n_{i,1} + H^n_{i-1,1} \right) \\ &+ \eta \left(H^n_{i,2} - H^n_{i,1} - (\Delta y) H_S \right) + \omega \left(\frac{Q^n_{i,1}}{\Delta x \Delta y H^n_{i,1}} \right). \end{aligned} \tag{26}$$

For $i = I - 1$ and $j = 4$ at $t > 0$, substituting the unknown value on the east boundary by backward difference approximation $H^n_{I,1} = H^n_{I-1,1} + (\Delta x) H_E$ and substituting the unknown value on the south boundary by forward difference approximation $H^n_{I-1,0} = H^n_{I-1,1} - (\Delta y) H_S$,

$$\begin{aligned} H^{n+1}_{I-1,1} &= H^n_{I-1,1} \\ &+ \xi \left((\Delta x) H_E - H^n_{I-1,1} + H^n_{I-2,1} \right) \\ &+ \eta \left(H^n_{I-1,2} - H^n_{I-1,1} - (\Delta y) H_S \right) \\ &+ \omega \left(\frac{Q^n_{I-1,1}}{\Delta x \Delta y H^n_{I-1,1}} \right). \end{aligned} \tag{27}$$

For $i = 1$ and $1 < j < J - 1$ at $t > 0$, substituting the known value on the west boundary by $H^n_{0,j} = H_1$,

$$\begin{aligned} H^{n+1}_{1,j} &= H^n_{1,j} + \xi \left(H^n_{2,j} - 2H^n_{1,j} + H_1 \right) \\ &+ \eta \left(H^n_{1,j+1} - 2H^n_{1,j} + H^n_{1,j-1} \right) + \omega \left(\frac{Q^n_{1,j}}{\Delta x \Delta y H^n_{1,j}} \right). \end{aligned} \tag{28}$$

For $i = I - 1$ and $1 < j < J - 1$ at $t > 0$, substituting the unknown value on the east boundary by backward difference approximation $H^n_{I,j} = H^n_{I-1,j} + (\Delta x) H_E$,

$$\begin{aligned} H^{n+1}_{I-1,j} &= H^n_{I-1,j} \\ &+ \xi \left((\Delta x) H_E - H^n_{I-1,j} + H^n_{I-2,j} \right) \\ &+ \eta \left(H^n_{I-1,j+1} - 2H^n_{I-1,j} + H^n_{I-1,j-1} \right). \\ &+ \omega \left(\frac{Q^n_{I-1,j}}{\Delta x \Delta y H^n_{I-1,j}} \right). \end{aligned} \tag{29}$$

For $i = 1$ and $j = J - 1$ at $t > 0$, substituting the known value on the west boundary by $H^n_{0,J-1} = H_1$ and substituting the unknown value on the north boundary by backward difference approximation $H^n_{1,J} = H^n_{1,J-1} + (\Delta y) H_N$,

$$\begin{aligned} H^{n+1}_{1,J-1} &= H^n_{1,J-1} \\ &+ \xi \left(H^n_{2,J-1} - 2H^n_{1,J-1} + H_1 \right) \\ &+ \eta \left((\Delta y) H_N - H^n_{1,J-1} + H^n_{1,J-2} \right) \\ &+ \omega \left(\frac{Q^n_{1,J-1}}{\Delta x \Delta y H^n_{1,J-1}} \right). \end{aligned} \tag{30}$$

For $< i < I - 1$ and $j = J - 1$ at $t > 0$, substituting the unknown value on the north boundary by backward difference approximation $H^n_{i,J} = H^n_{i,J-1} + (\Delta y) H_N$,

$$\begin{aligned} H^{n+1}_{i,J-1} &= H^n_{i,J-1} \\ &+ \xi \left(H^n_{i+1,J-1} - 2H^n_{i,J-1} + H^n_{i-1,J-1} \right) \\ &+ \eta \left((\Delta y) H_N - H^n_{i,J-1} + H^n_{i,J-2} \right) \\ &+ \omega \left(\frac{Q^n_{i,J-1}}{\Delta x \Delta y H^n_{i,J-1}} \right). \end{aligned} \tag{31}$$

For $i = I - 1$ and $j = J - 1$ at $t > 0$, substituting the unknown value on the east boundary by backward difference approximation $H^n_{I,J-1} = H^n_{I-1,J-1} + (\Delta x) H_E$ and substituting the unknown value on the north boundary by backward difference approximation $H^n_{I-1,J} = H^n_{I-1,J-1} + (\Delta y) H_N$,

$$\begin{aligned} H^{n+1}_{I-1,J-1} &= H^n_{I-1,J-1} \\ &+ \xi \left((\Delta x) H_E - H^n_{I-1,J-1} + H^n_{I-2,J-1} \right) \\ &+ \eta \left((\Delta y) H_N - H^n_{I-1,J-1} + H^n_{I-1,J-2} \right) \\ &+ \omega \left(\frac{Q^n_{I-1,J-1}}{\Delta x \Delta y H^n_{I-1,J-1}} \right). \end{aligned} \tag{32}$$

B. Finite Difference Method for the Flow Velocity Model

We will propose the forward time central space method (FTCS) to the transient groundwater model. We discretize equations (11) and (12) by dividing the interval $[0, L]$ in x-direction into I subintervals such that $I\Delta x = L$, the interval $[0, M]$ in y-direction into J subintervals such that $J\Delta y = M$ and the interval $[0, T]$ in time into N subintervals such that $N\Delta t = T$. We can then approximate $U(x, y, t)$ by $U^n_{i,j}$ and $V(x, y, t)$ by $V^n_{i,j}$, value of the difference approximation of $U(x, y, t)$ and $V(x, y, t)$ at point $x = i\Delta x$, $y = j\Delta y$ and $x = n\Delta t$ where $0 \leq i \leq I$, $0 \leq j \leq J$ and $0 \leq n \leq N$ which i, j and n are positive integers.

Taking the forward difference scheme in space in each terms of equations (11) and (12), then

$$U^n_{i,j} = -K \left(\frac{H^n_{i+1,j} - H^n_{i,j}}{\Delta x} \right), \tag{33}$$

$$V_{i,j}^{n} = -K\left(\frac{H_{i,j+1}^{n} - H_{i,j}^{n}}{\Delta y}\right). \tag{34}$$

Taking the backward difference scheme in space in each terms ofequations(11) and (12), then

$$U_{i,j}^{n} = -K\left(\frac{H_{i,j}^{n} - H_{i-1,j}^{n}}{\Delta x}\right), \tag{35}$$

$$V_{i,j}^{n} = -K\left(\frac{H_{i,j}^{n} - H_{i,j-1}^{n}}{\Delta y}\right). \tag{36}$$

C. Finite Difference Method for the Dispersion Model

We will propose the forward time central space method (FTCS) to the transient groundwater model. We discretize equation (13) by dividing the interval $[0, L]$ in x-direction into I subintervals such that $I\Delta x = L$, the interval $[0, M]$ in y-direction into J subintervals such that $J\Delta y = M$ and the interval $[0, T]$ in time into N subintervals such that $N\Delta t = T$. We can then approximate $C(x, y, t)$ by $C_{i,j}^{n}$, value of the difference approximation of $C(x, y, t)$ at point $x = i\Delta x$, $y = j\Delta y$ and $x = n\Delta t$ where $0 \leq i \leq I$, $0 \leq j \leq J$ and $0 \leq n \leq N$ which i, j and n are positive integers.

Taking the central difference scheme in space and forward difference scheme in time into each terms of equation (13), then

$$\frac{\partial^2 C}{\partial x^2} = \frac{C_{i+1,j}^{n} - 2C_{i,j}^{n} + C_{i-1,j}^{n}}{(\Delta x)^2}, \tag{37}$$

$$\frac{\partial^2 C}{\partial y^2} = \frac{C_{i,j+1}^{n} - 2C_{i,j}^{n} + C_{i,j-1}^{n}}{(\Delta y)^2}, \tag{38}$$

$$\frac{\partial C}{\partial x} = \frac{C_{i+1,j}^{n} - C_{i-1,j}^{n}}{2\Delta x}, \tag{39}$$

$$\frac{\partial C}{\partial y} = \frac{C_{i,j+1}^{n} - C_{i,j-1}^{n}}{2\Delta y}, \tag{40}$$

$$\frac{\partial C}{\partial t} = \frac{C_{i,j}^{n+1} - C_{i,j}^{n}}{\Delta t}. \tag{41}$$

Substituting equations (37) – (38) into equation (10), for $1 < i < I - 1$ and $1 < j < J - 1$ at $t > 0$,

$$\begin{aligned} C_{i,j}^{n+1} &= (a_1 - a_3)\, C_{i+1,j}^{n} \\ &+ (1 - 2a_1 - 2a_2)\, C_{i,j}^{n} \\ &+ (a_1 + a_3)\, C_{i-1,j}^{n} \\ &+ (a_2 - a_4)\, C_{i,j+1}^{n} \\ &+ (a_2 + a_4)\, C_{i,j-1}^{n}, \end{aligned} \tag{42}$$

where $a_1 = \frac{D_x \Delta t}{(\Delta x)^2}$, $a_2 = \frac{D_y \Delta t}{(\Delta y)^2}$, $a_3 = \frac{U_{i,j} \Delta t}{2\Delta x}$, $a_4 = \frac{V_{i,j} \Delta t}{2\Delta y}$ and $a_5 = v\Delta t$.

For $i = 1$ and $j = 1$ at $t > 0$, substituting the known value on the west boundary by $C_{0,1}^{n} = C_1$, substituting the unknown value on the south boundary by forward difference approximation $C_{1,0}^{n} = C_{1,1}^{n} - (\Delta y)\, C_S$,

$$\begin{aligned} C_{1,1}^{n+1} &= (a_1 - a_3)\, C_{2,1}^{n} \\ &+ (a_1 + a_3)\, C_1 \\ &+ (a_2 - a_4)\, C_{1,2}^{n} \\ &+ (1 - 2a_1 - a_2 + a_4 - a_5)\, C_{1,1}^{n} \\ &- (a_2 + a_4)\, (\Delta y)\, H_S. \end{aligned} \tag{43}$$

For $1 < i < I - 1$ and $j = 1$ at $t > 0$, substituting the unknown value on the south boundary by forward difference approximation $C_{i,0}^{n} = C_{i,1}^{n} - (\Delta y)\, C_S$,

$$\begin{aligned} C_{i,1}^{n+1} &= (a_1 - a_3)\, C_{i+1,1}^{n} \\ &+ (a_1 + a_3)\, C_{i-1,1}^{n} \\ &+ (a_2 - a_4)\, C_{i,2}^{n} \\ &+ (1 - 2a_1 - a_2 + a_4 - a_5)\, C_{i,1}^{n} \\ &- (a_2 + a_4)\, (\Delta y)\, B_S. \end{aligned} \tag{44}$$

For $i = I - 1$ and $j = J - 1$ at $t > 0$, substituting the unknown value on the east boundary by backward difference approximation $C_{I,1}^{n} = C_{I-1,1}^{n} + (\Delta x)\, C_E$ and substituting the unknown value on the south boundary by forward difference $C_{I-1,0}^{n} = C_{I-1,1}^{n} - (\Delta y)\, C_S$,

$$\begin{aligned} C_{I-1,1}^{n+1} &= (a_1 + a_3)\, C_{I-2,1}^{n} \\ &+ (a_2 - a_4)\, C_{I-1,2}^{n} \\ &+ (1 - a_1 - a_2 - a_3 + a_4 - a_5)\, C_{I-1,1}^{n} \\ &+ (a_1 - a_3)\, (\Delta x)\, H_E \\ &- (a_2 + a_4)\, (\Delta y)\, H_S. \end{aligned} \tag{45}$$

For $i = 1$ and $1 < j < J - 1$ at $t > 0$, substituting the known value on the west boundary by $C_{0,j}^{n} = C_1$,

$$\begin{aligned} C_{1,j}^{n+1} &= (a_1 - a_3)\, C_{2,j}^{n} \\ &+ (a_1 + a_3)\, C_1 \\ &+ (a_2 - a_4)\, C_{1,j+1}^{n} \\ &+ (a_2 + a_4)\, C_{1,j-1}^{n} \\ &+ (1 - 2a_1 - 2a_2 - a_5)\, C_{1j}^{n}. \end{aligned} \tag{46}$$

For $i = I - 1$ and $1 < j < J - 1$ at $t > 0$, substituting the unknown value on the east boundary by backward difference approximation $C_{I,j}^{n} = C_{I-1,j}^{n} + (\Delta x)\, C_E$,

$$\begin{aligned} C_{I-1,j}^{n+1} &= (a_1 + a_3)\, C_{I-2,j}^{n} \\ &+ (a_2 - a_4)\, C_{I-1,j+1}^{n} \\ &+ (a_2 + a_4)\, C_{I-1,j-1}^{n} \\ &+ (1 - a_1 - 2a_2 - a_3 - a_5)\, C_{I-1,j}^{n} \\ &+ (a_1 - a_3)\, (\Delta x)\, H_E. \end{aligned} \tag{47}$$

For $i = 1$ and $j = J - 1$ at $t > 0$, substituting the known value on the west boundary by $C_{0,J-1}^{n} = C_1$ and substituting the unknown value on the north boundary by backward difference $C_{1,J}^{n} = C_{1,J-1}^{n} + (\Delta y)\, C_N$,

$$\begin{aligned} C_{1,J-1}^{n+1} &= (a_1 - a_3)\, C_{2,J-1}^{n} \\ &+ (a_1 + a_3)\, C_1 \\ &+ (a_2 + a_4)\, C_{1,J-2}^{n} \\ &+ (1 - 2a_1 - a_2 - a_4 - a_5)\, C_{1,J-1}^{n} \\ &+ (a_2 - a_4)\, (\Delta y)\, H_N. \end{aligned} \tag{48}$$

For $1 < i < I - 1$ and $j = J - 1$ at $t > 0$, substituting the unknown value on the north boundary by backward difference approximation $C_{i,J}^{n} = C_{i,J-1}^{n} + (\Delta y)\, C_N$,

$$\begin{aligned} C_{i,J-1}^{n+1} &= (a_1 - a_3)\, C_{i+1,J-1}^{n} \\ &+ (a_1 + a_3)\, C_{i-1,J-1}^{n} \\ &+ (a_2 + a_4)\, C_{i,J-2}^{n} \\ &+ (1 - 2a_1 - a_2 - a_4 - a_5)\, C_{i,J-1}^{n} \\ &+ (a_2 - a_4)\, (\Delta y)\, H_N. \end{aligned} \tag{49}$$

For $i = I - 1$ and $j = J - 1$ at $t > 0$, substituting the unknown value on the east boundary by backward difference

approximation $C^n_{I,J-1} = C^n_{I-1,J-1} + (\Delta x)\, C_E$ and substituting the unknown value on the north boundary by backward difference approximation $C^n_{I-1,J} = C^n_{I-1,J-1} + (\Delta y)\, C_N$,

$$\begin{aligned} C^{n+1}_{I-1,J-1} &= (a_1 + a_3)\, C^n_{I-2,J-1} \\ &+ (a_2 + a_4)\, C^n_{I-1,J-2} \\ &+ (1 - a_1 - a_2 - a_3 - a_4 - a_5)\, C^n_{I-1,J-1} \\ &+ (a_1 - a_3)\, (\Delta x)\, H_E \\ &+ (a_2 - a_4)\, (\Delta y)\, H_N. \end{aligned} \tag{50}$$

IV. Numerical Experiment

The groundwater flow models provide hydraulic head. The computed hydraulic head is transformed to be groundwater flow velocity by using the flow velocity model. The results from the flow velocity model will input the dispersion model that provide groundwater pollutant concentration. We assume the experimented vertically area around waste landfill has dimension that 2.4 km $\times$ 2.4 km. The experimented area has homogeneous aquifer parameters, the hydraulic conductivity $K = 15\ m/day$, storage capacity $S = 1\ m^{-1}$, diffusion coefficients $D_x = D_y = 0.2\ m^2/day$, grid spacing $\Delta x = \Delta y = 100$ m and time step $\Delta t = 0.1$ day.

A. Simulation 1 : Low Level of Difference Hydraulic Head

The initial and boundary conditions of groundwater flow model are specified Eqs.(3) - (8) where $H_Z = 25$, $H_0 = 15$, $H_N = 0$, $H_S = 0$ and $H_E = 0$. The initial and boundary conditions of dispersion model are specified Eqs.(14) - (19) where $C_Z = 1$, $C_0 = 0$, $C_N = 0$, $C_S = 0$ and $C_E = 0$. There is no injection wells. The finite difference method are used to approximate solution of three models, the results of hydraulic head, velocity flow and groundwater pollutant are shown in Table I - III, respectively. And the line graphs of hydraulic head, velocity in x - direction and groundwater pollutant concentration are shown Figure 1 - 3, respectively.

TABLE I
Hydraulic Head at $t = 3600$ Day of Simulation 1

y/x	400	800	1200	1600	2000	2400
0	22.0026	19.4154	17.4907	16.2680	15.6407	15.4825
400	22.0026	19.4154	17.4907	16.2680	15.6407	15.4825
800	22.0026	19.4154	17.4907	16.2680	15.6407	15.4825
1200	22.0026	19.4154	17.4907	16.2680	15.6407	15.4825
1600	22.0026	19.4154	17.4907	16.2680	15.6407	15.4825
2000	22.0026	19.4154	17.4907	16.2680	15.6407	15.4825
2400	22.0026	19.4154	17.4907	16.2680	15.6407	15.4825

TABLE II
Velocity Flow in x-direction at $t = 3600$ Day of Simulation 1

y/x	400	800	1200	1600	2000	2400
0	0.1088	0.0886	0.0620	0.0367	0.0163	0.0039
400	0.1088	0.0886	0.0620	0.0367	0.0163	0.0039
800	0.1088	0.0886	0.0620	0.0367	0.0163	0.0039
1200	0.1088	0.0886	0.0620	0.0367	0.0163	0.0039
1600	0.1088	0.0886	0.0620	0.0367	0.0163	0.0039
2000	0.1088	0.0886	0.0620	0.0367	0.0163	0.0039
2400	0.1088	0.0886	0.0620	0.0367	0.0163	0.0039

TABLE III
Ground Pollutant Concentration at $t = 3600$ Day of Simulation 1

y/x	400	800	1200	1600	2000	2400
0	1.0148	1.0153	1.0000	1.1143	0.0826	0.0003
400	1.0148	1.0153	1.0000	1.1143	0.0826	0.0003
800	1.0148	1.0153	1.0000	1.1143	0.0826	0.0003
1200	1.0148	1.0153	1.0000	1.1143	0.0826	0.0826
1600	1.0148	1.0153	1.0000	1.1143	0.0826	0.0826
2000	1.0148	1.0153	1.0000	1.1143	0.0826	0.0826
2400	1.0148	1.0153	1.0000	1.1143	0.0826	0.0826

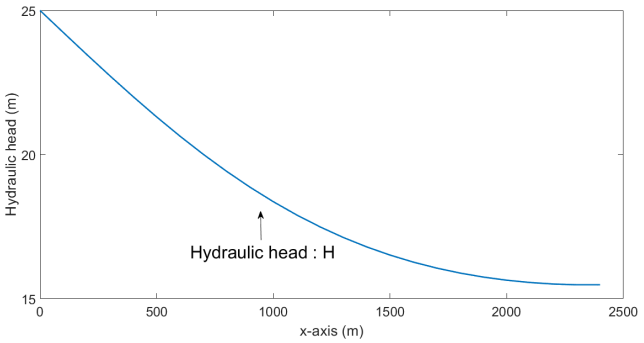

Fig. 1. The line graph of hydraulic head of simulation 1 at $t = 3600$ day and $y = 1200$ m

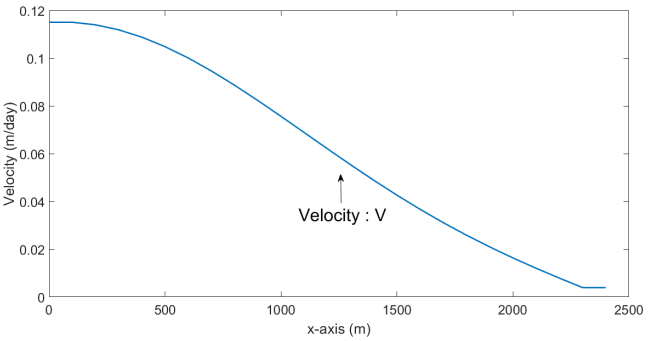

Fig. 2. The line graph of velocity in x - direction of simulation 1 at $t = 3600$ day and $y = 1200$ m

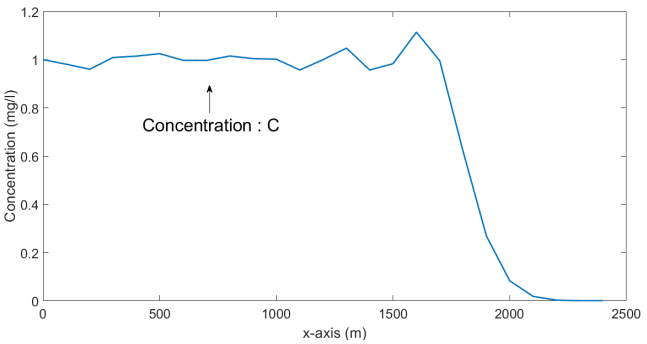

Fig. 3. The line graph of groundwater pollutant concentration of simulation 1 at $t = 3600$ day and $y = 1200$ m

B. Simulation 2 : High Level of Difference Hydraulic Head

The initial and boundary conditions of groundwater flow model are specified Eqs.(3) - (8) where $H_Z = 25$, $H_0 = 10$, $H_N = 0$, $H_S = 0$ and $H_E = 0$. The initial and boundary

conditions of dispersion model are specified Eqs.(14) - (19) where $C_Z = 1$, $C_0 = 0$, $C_N = 0$, $C_S = 0$ and $C_E = 0$. There is no injection wells. The finite difference method are used to approximate solution of three models, the results of hydraulic head, velocity flow and groundwater pollutant are shown in Table IV - VI, respectively. And the line graph of groundwater pollutant concentration is shown Figure 4.

TABLE IV
HYDRAULIC HEAD AT $t = 3600$ DAY OF SIMULATION 2

y/x	400	800	1200	1600	2000	2400
0	20.5039	16.6231	13.7361	11.9019	10.9611	10.7237
400	20.5039	16.6231	13.7361	11.9019	10.9611	10.7237
800	20.5039	16.6231	13.7361	11.9019	10.9611	10.7237
1200	20.5039	16.6231	13.7361	11.9019	10.9611	10.7237
1600	20.5039	16.6231	13.7361	11.9019	10.9611	10.7237
2000	20.5039	16.6231	13.7361	11.9019	10.9611	10.7237
2400	20.5039	16.6231	13.7361	11.9019	10.9611	10.7237

TABLE V
VELOCITY FLOW IN X-DIRECTION AT $t = 3600$ DAY OF SIMULATION 2

y/x	400	800	1200	1600	2000	2400
0	0.1725	0.1632	0.1329	0.0930	0.0245	0.0058
400	0.1725	0.1632	0.1329	0.0930	0.0245	0.0058
800	0.1725	0.1632	0.1329	0.0930	0.0245	0.0058
1200	0.1725	0.1632	0.1329	0.0930	0.0245	0.0058
1600	0.1725	0.1632	0.1329	0.0930	0.0245	0.0058
2000	0.1725	0.1632	0.1329	0.0930	0.0245	0.0058
2400	0.1725	0.1632	0.1329	0.0930	0.0245	0.0058

TABLE VI
GROUND POLLUTANT CONCENTRATION AT $t = 3600$ DAY OF SIMULATION 2

y/x	400	800	1200	1600	2000	2400
0	0.9409	1.0170	1.0162	0.9405	0.4822	0.0056
400	0.9409	1.0170	1.0162	0.9405	0.4822	0.0056
800	0.9409	1.0170	1.0162	0.9405	0.4822	0.0056
1200	0.9409	1.0170	1.0162	0.9405	0.4822	0.0056
1600	0.9409	1.0170	1.0162	0.9405	0.4822	0.0056
2000	0.9409	1.0170	1.0162	0.9405	0.4822	0.0056
2400	0.9409	1.0170	1.0162	0.9405	0.4822	0.0056

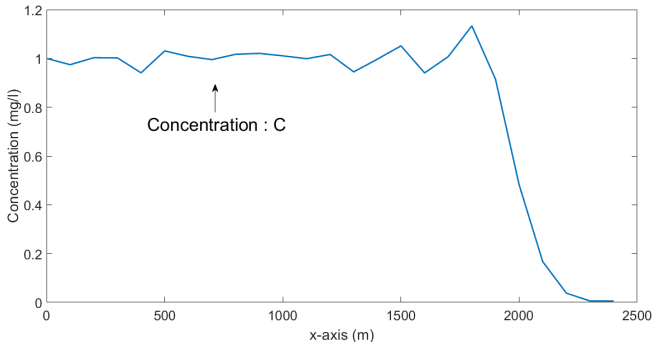

Fig. 4. The line graph of groundwater pollutant concentration of simulation 2 at $t = 3600$ day and $y = 1200$ m

C. Simulation 3 : High Level of Difference Hydraulic Head with Five Injection Wells

The initial and boundary conditions of groundwater flow model are specified Eqs.(3) - (8) where $H_Z = 25$, $H_0 = 10$, $H_N = 0$, $H_S = 0$ and $H_E = 0$. The initial and boundary conditions of dispersion model are specified Eqs.(14) - (19) where $C_Z = 1$, $C_0 = 0$, $C_N = 0$, $C_S = 0$ and $C_E = 0$. There is five injection wells where $Q(800, 400) = Q(800, 800) = Q(800, 1200) = Q(8000, 1600) = Q(800, 2000) = -105\ m^3/day$. The finite difference method are used to approximate solution of three models, the results of hydraulic head, velocity flow and groundwater pollutant are shown in Table VII - IX, respectively. And the line graph of groundwater pollutant concentration is shown Figure 5.

TABLE VII
HYDRAULIC HEAD AT $t = 3600$ DAY OF SIMULATION 3

y/x	400	800	1200	1600	2000	2400
0	20.3233	16.3162	13.4886	11.7465	10.8647	10.6437
400	20.3094	16.1304	13.4737	11.7431	10.8636	10.6430
800	20.2929	16.0973	13.4551	11.7362	10.8609	10.6412
1200	20.2876	16.0887	13.4487	11.7331	10.8596	10.6402
1600	20.2929	16.0973	13.4551	11.7362	10.8609	10.6412
2000	20.3094	16.1304	13.4737	11.7431	10.8636	10.6430
2400	20.3233	16.3162	13.4886	11.7465	10.8647	10.6437

TABLE VIII
VELOCITY FLOW IN X-DIRECTION AT $t = 3600$ DAY OF SIMULATION 3

y/x	400	800	1200	1600	2000	2400
0	0.1698	0.1355	0.0895	0.0519	0.0228	0.0054
400	0.1706	0.1511	0.0881	0.0517	0.0228	0.0054
800	0.1713	0.1514	0.0874	0.0514	0.0227	0.0054
1200	0.1715	0.1515	0.0873	0.0513	0.0226	0.0054
1600	0.1713	0.1514	0.0874	0.0514	0.0227	0.0054
2000	0.1706	0.1511	0.0881	0.0517	0.0228	0.0054
2400	0.1698	0.1355	0.0895	0.0519	0.0228	0.0054

TABLE IX
GROUND POLLUTANT CONCENTRATION AT $t = 3600$ DAY OF SIMULATION 3

y/x	400	800	1200	1600	2000	2400
0	0.9691	1.0059	0.9952	0.9331	0.3656	0.0033
400	0.9825	1.0047	0.9845	0.9334	0.3519	0.0030
800	0.9917	1.0068	0.9797	0.9347	0.3391	0.0028
1200	0.9941	1.0076	0.9787	0.9354	0.3352	0.0028
1600	0.9920	1.0068	0.9796	0.9347	0.3391	0.0028
2000	0.9831	1.0040	0.9841	0.9333	0.3519	0.0030
2400	0.9690	1.0059	0.9956	0.9330	0.3659	0.0033

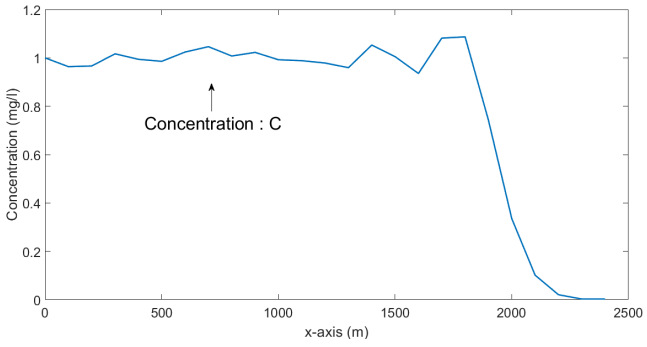

Fig. 5. The line graph of groundwater pollutant concentration of simulation 3 at $t = 3600$ day and $y = 1200$ m

D. Simulation 4 : High Level of Difference Hydraulic Head with Fifteen Injection Wells

The initial and boundary conditions of groundwater flow model are specified Eqs.(3) - (8) where $H_Z = 25$, $H_0 = 10$, $H_N = 0$, $H_S = 0$ and $H_E = 0$. The initial and boundary conditions of dispersion model are specified Eqs.(14) - (19) where $C_Z = 1$, $C_0 = 0$, $C_N = 0$, $C_S = 0$ and $C_E = 0$. There is five injection wells where $Q(800, 400) = Q(800, 800) = Q(800, 1200) = Q(8000, 1600) = Q(800, 2000) = Q(1200, 400) = Q(1200, 800) = Q(1200, 1200) = Q(12000, 1600) = Q(1200, 2000) = Q(1600, 400) = Q(1600, 800) = Q(1600, 1200) = Q(16000, 1600) = Q(1600, 2000) = -105\ m^3/day$. The finite difference method are used to approximate solution of three models, the results of hydraulic head, velocity flow and groundwater pollutant are shown in Table X - XII, respectively. And the line graph of groundwater pollutant concentration is shown Figure 6.

TABLE X
HYDRAULIC HEAD AT $t = 3600$ DAY OF SIMULATION 4

y/x	400	800	1200	1600	2000	2400
0	20.0922	15.8057	12.6911	10.8856	10.1626	10.0094
400	20.0725	15.5890	12.4108	10.5782	10.1321	9.9937
800	20.0443	15.5196	12.3169	10.4914	10.0862	9.9615
1200	20.0339	15.4977	12.2879	10.4646	10.0685	0.9472
1600	20.0443	15.5196	12.3169	10.4914	10.0862	9.9615
2000	20.0725	15.5890	12.4108	10.5782	10.1321	9.9937
2400	20.0922	15.8057	12.6911	10.8856	10.1626	10.0094

TABLE XI
VELOCITY FLOW IN X-DIRECTION $t = 3600$ DAY OF SIMULATION 4

y/x	400	800	1200	1600	2000	2400
0	0.1789	0.1468	0.0985	0.0506	0.0167	0.0037
400	0.1800	0.1642	0.1186	0.0725	0.0144	0.0034
800	0.1813	0.1657	0.1193	0.0719	0.0130	0.0030
1200	0.1817	0.1662	0.1195	0.0718	0.0127	0.0029
1600	0.1813	0.1657	0.1193	0.0719	0.0130	0.0030
2000	0.1800	0.1642	0.1186	0.0725	0.0144	0.0034
2400	0.1789	0.1468	0.0985	0.0506	0.0167	0.0037

TABLE XII
GROUND POLLUTANT CONCENTRATION AT $t = 3600$ DAY OF SIMULATION 4

y/x	400	800	1200	1600	2000	2400
0	0.9977	0.9861	1.0596	0.9282	0.1951	0.0008
400	1.0179	1.0172	1.1214	1.0233	0.0897	0.0003
800	1.0254	1.0221	1.1402	1.0570	0.0645	0.0002
1200	1.0262	1.0227	1.1451	1.0703	0.0596	0.0001
1600	1.0263	1.0235	1.1441	1.0667	0.0639	0.0002
2000	1.0213	1.0217	1.1329	1.0421	0.0880	0.0003
2000	0.9966	0.9855	1.0586	0.9297	0.1963	0.0008

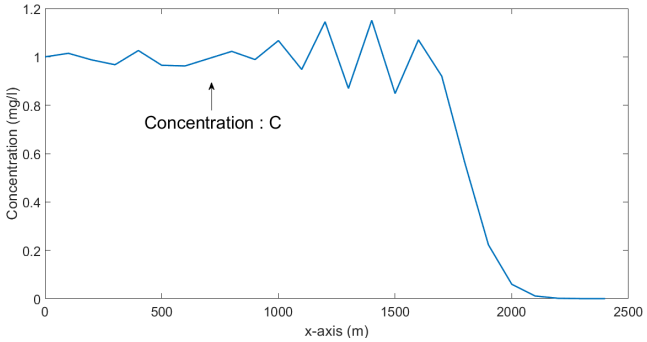

Fig. 6. The line graph of groundwater pollutant concentration of simulation 4 at $t = 3600$ day and $y = 1200$ m

E. Simulation 5 : High Level of Difference Hydraulic Head with Five Injection Wells and Ascending Hydraulic Conductivity

The initial and boundary conditions of groundwater flow model are specified Eqs.(3) - (8) where $H_Z = 25$, $H_0 = 10$, $H_N = 0$, $H_S = 0$ and $H_E = 0$. The initial and boundary conditions of dispersion model are specified Eqs.(14) - (19) where $C_Z = 1$, $C_0 = 0$, $C_N = 0$, $C_S = 0$ and $C_E = 0$. There is five injection wells where $Q(800, 400) = Q(800, 800) = Q(800, 1200) = Q(8000, 1600) = Q(800, 2000) = -105\ m^3/day$. The ascending hydraulic conductivity is given each area in Table XIII. The finite difference method are used to approximate solution of three models, the results of hydraulic head, velocity flow and groundwater pollutant are shown in Table XIV - XVI, respectively. And the line graph of groundwater pollutant concentration is shown Figure 7.

TABLE XIII
HYDRAULIC CONDUCTIVITY OF SIMULATION 5

y/x	400	800	1200	1600	2000	2400
0	10	13	15	30	40	40
400	10	14	15	30	40	40
800	10	13	15	30	40	40
1200	10	14	15	30	40	40
1600	10	13	15	30	40	40
2000	10	14	15	30	40	40
2400	11	13	15	30	40	40

TABLE XIV
HYDRAULIC HEAD AT $t = 3600$ DAY OF SIMULATION 5

y/x	400	800	1200	1600	2000	2400
0	19.9454	15.8959	13.3319	12.0446	11.4591	11.3073
400	19.9253	15.6879	13.3137	12.0400	11.4502	11.3061
800	19.8993	15.6258	13.2879	12.0301	11.4460	11.3031
1200	19.8883	15.6307	13.2783	12.0247	11.4432	11.3009
1600	19.8876	15.6156	13.2820	12.0267	11.4437	11.3011
2000	19.9183	15.6723	13.3037	12.0342	11.4463	11.3028
2400	19.9411	15.8799	13.3215	12.0381	11.4475	11.3035

TABLE XV
VELOCITY FLOW IN X-DIRECTION AT $t = 3600$ DAY OF SIMULATION 5

y/x	400	800	1200	1600	2000	2400
0	0.1319	0.1239	0.0763	0.0709	0.0389	0.0096
400	0.1205	0.1400	0.0748	0.0704	0.0387	0.0096
800	0.1212	0.1314	0.0738	0.0696	0.0384	0.0095
1200	0.1213	0.1403	0.0737	0.0693	0.0382	0.0095
1600	0.1214	0.1314	0.0736	0.0694	0.0383	0.0095
2000	0.1329	0.1400	0.0745	0.0701	0.0386	0.0095
2400	0.1322	0.1151	0.0761	0.0706	0.0387	0.0095

TABLE XVI
GROUND POLLUTANT CONCENTRATION AT $t = 3600$ DAY OF SIMULATION 5

y/x	400	800	1200	1600	2000	2400
0	0.9995	1.0138	1.0331	0.9514	0.7021	0.0166
400	0.9913	1.0184	1.0200	0.9518	0.6630	0.0148
800	0.9801	1.0166	1.0114	0.9475	0.6208	0.0129
1200	0.9792	1.0099	1.0100	0.9466	0.6089	0.0124
1600	0.9703	0.9827	0.9988	0.9466	0.6105	0.0125
2000	0.9797	1.0127	1.0177	0.9500	0.6512	0.0143
2400	1.0060	1.0171	1.0367	0.9491	0.6936	0.0162

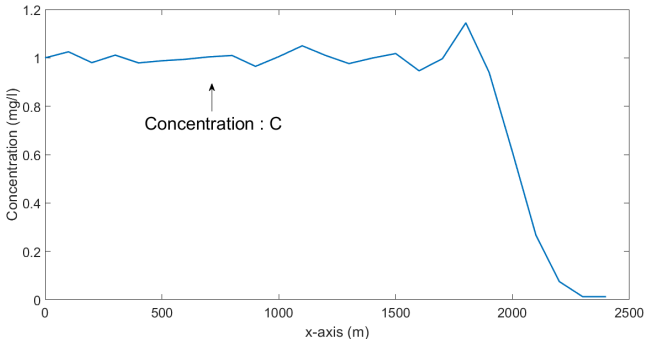

Fig. 7. The line graph of groundwater pollutant concentration of simulation 5 at $t = 3600$ day and $y = 1200$ m

F. Simulation 6 : High Level of Difference Hydraulic Head with Five Injection Wells and Descending Hydraulic conductivity

The initial and boundary conditions of groundwater flow model are specified Eqs.(3) - (8) where $H_Z = 25$, $H_0 = 10$, $H_N = 0$, $H_S = 0$ and $H_E = 0$. The initial and boundary conditions of dispersion model are specified Eqs.(14) - (19) where $C_Z = 1$, $C_0 = 0$, $C_N = 0$, $C_S = 0$ and $C_E = 0$. There is five injection wells where $Q(800, 400) = Q(800, 800) = Q(800, 1200) = Q(8000, 1600) = Q(800, 2000) = -105\ m^3/day$. The descending hydraulic conductivity is given each area in Table XVII. The finite difference method are used to approximate solution of three models, the results of hydraulic head, velocity flow and groundwater pollutant are shown in Table XVIII - XX, respectively. And the line graph of groundwater pollutant concentration is shown Figure 8.

TABLE XVII
HYDRAULIC CONDUCTIVITY OF SIMULATION 6

y/x	400	800	1200	1600	2000	2400
0	40	30	15	13	10	10
400	40	30	15	14	10	10
800	40	30	15	13	10	10
1200	40	30	15	14	10	10
1600	40	30	15	13	10	10
2000	40	30	15	14	11	11
2400	40	30	15	13	10	10

TABLE XVIII
HYDRAULIC HEAD AT $t = 3600$ DAY OF SIMULATION 6

y/x	400	800	1200	1600	2000	2400
0	21.2287	17.6561	14.6074	12.4399	11.1912	10.8511
400	21.2225	17.5707	14.5993	12.4371	11.1815	10.8390
800	21.2152	17.5559	14.5904	12.4304	11.1757	10.8328
1200	21.2127	17.5518	14.5870	12.4301	11.1699	10.8243
1600	21.2147	17.5547	14.5879	12.4249	11.1653	10.8205
2000	21.2217	17.5687	14.5951	12.4293	11.1789	10.8391
2400	21.2278	17.6535	14.6018	12.4311	11.1870	10.8501

TABLE XIX
VELOCITY FLOW IN X-DIRECTION AT $t = 3600$ DAY OF SIMULATION 6

y/x	400	800	1200	1600	2000	2400
0	0.3736	0.2575	0.1027	0.0636	0.0257	0.0062
400	0.3766	0.2719	0.1021	0.0635	0.0236	0.0056
800	0.3754	0.2721	0.1018	0.0589	0.0235	0.0056
1200	0.3757	0.2722	0.1017	0.0634	0.0238	0.0057
1600	0.3755	0.2722	0.1019	0.0590	0.0237	0.0057
2000	0.3747	0.2720	0.1022	0.0636	0.0256	0.0061
2400	0.3737	0.2576	0.1028	0.0591	0.0253	0.0061

TABLE XX
GROUND POLLUTANT CONCENTRATION AT $t = 3600$ DAY OF SIMULATION 6

y/x	400	800	1200	1600	2000	2400
0	0.9881	0.9722	0.9812	0.9997	1.0304	0.0435
400	0.9867	0.9637	0.9836	0.9995	1.0105	0.0396
800	0.9899	0.9613	0.9828	1.0081	0.9965	0.0383
1200	0.9909	0.9599	0.9855	0.9989	1.0124	0.0392
1600	0.9902	0.9616	0.9821	1.0083	0.9871	0.0358
2000	0.9865	0.9631	0.9826	1.0033	1.0190	0.0415
2400	0.9889	0.9735	0.9779	1.0099	1.0068	0.0414

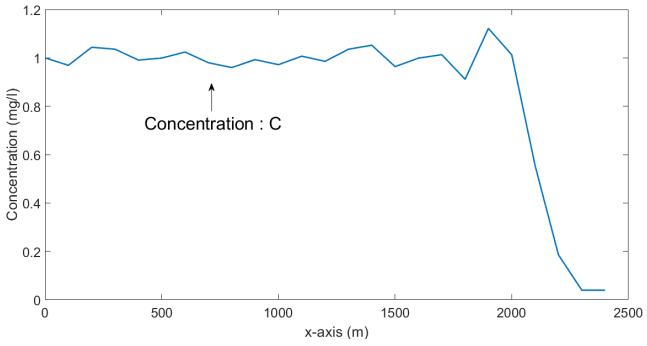

Fig. 8. The line graph of groundwater pollutant concentration of simulation 6 at $t = 3600$ day and $y = 1200$ m

G. Simulation 7 : Comparison Six Simulations

The all parameter of simulation 1 - 6 are shown in Table XXI. The comparison velocity flow in x-direction between

simulation 1 and 2 is shown in Figure 9. The comparison velocity flow in x-direction among simulation 2,3 and 4 is shown in Figure 10. The comparison velocity flow in x-direction between each derivative H_E is shown in Figure 11. The line graphs of velocity flow in x-direction of simulation 5 and 6 are shown in Figure 12 and 14, respectively. And the line graphs of hydraulic conductivity of simulation 5 and 6 are shown in Figure 13 and 15, respectively.

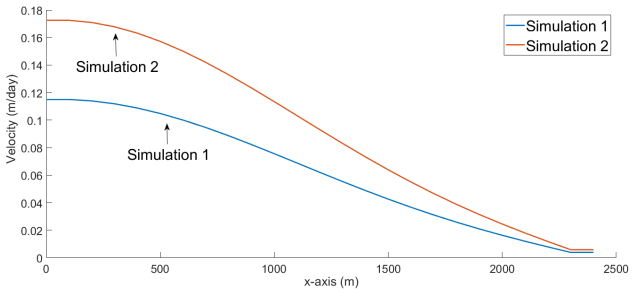

Fig. 9. Comparison flow velocity in x - direction of simulation 1 and 2 at $t = 3600$ day and $y = 1200$ m

TABLE XXI
THE BOUNDARY CONDITIONS AND PUMPING WELLS OF SIMULATION 1 - 6

Simulation	H_Z	H_0	H_N	H_S	H_E
1	25	15	0	0	0
2	25	10	0	0	0
3	25	10	0	0	0
4	25	10	0	0	0
5	25	10	0	0	0
6	25	10	0	0	0

Simulation	C_Z	C_0	C_N	C_S	C_E
1	1	0	0	0	0
2	1	0	0	0	0
3	1	0	0	0	0
4	1	0	0	0	0
5	1	0	0	0	0
6	1	0	0	0	0

Simulation	Q_1	Q_2	Q_3	Q_4	Q_5
1	0	0	0	0	0
2	0	0	0	0	0
3	-105	-105	-105	-105	-105
4	-105	-105	-105	-105	-105
5	-105	-105	-105	-105	-105
6	-105	-105	-105	-105	-105

Simultaion	Q_6	Q_7	Q_8	Q_9	Q_{10}
1	0	0	0	0	0
2	0	0	0	0	0
3	0	0	0	0	0
4	-105	-105	-105	-105	-105
5	0	0	0	0	0
6	0	0	0	0	0

Simulation	Q_{11}	Q_{12}	Q_{13}	Q_{14}	Q_{15}
1	0	0	0	0	0
2	0	0	0	0	0
3	0	0	0	0	0
4	-105	-105	-105	-105	-105
5	0	0	0	0	0
6	0	0	0	0	0

From the Table XXI, given $Q_1 = Q(800, 400)$, $Q_2 = Q(800, 800)$, $Q_3 = Q(800, 1200)$, $Q_4 = Q(800, 1600)$, $Q_5 = Q(800, 2000)$, $Q_6 = Q(1200, 400)$, $Q_7 = Q(1200, 800)$, $Q_8 = Q(1200, 1200)$, $Q_9 = Q(1200, 1600)$, $Q_{10} = Q(1200, 2000)$, $Q_{11} = Q(1600, 400)$, $Q_{12} = Q(1600, 800)$, $Q_{13} = Q(1600, 1200)$, $Q_{14} = Q(1600, 1600)$ and $Q_{15} = Q(1600, 2000)$.

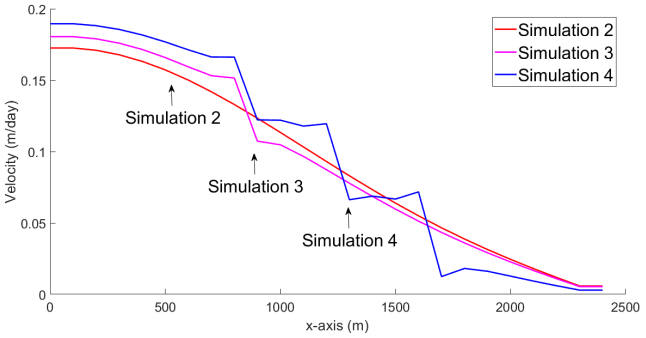

Fig. 10. Comparison flow velocity in x - direction of simulation 2, 3 and 4 at $t = 3600$ day and $y = 1200$ m

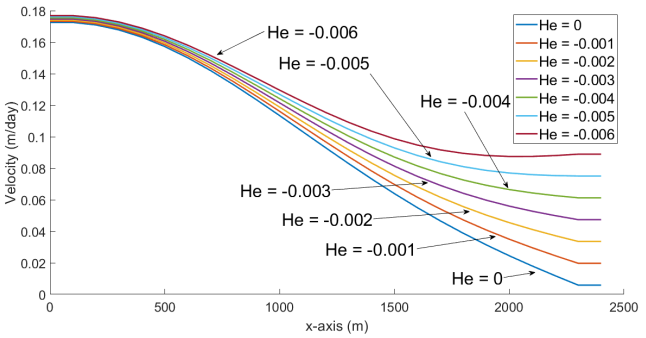

Fig. 11. Comparison flow velocity in x direction between different of derivative values H_E at $t = 3600$ day and $y = 1200$ m

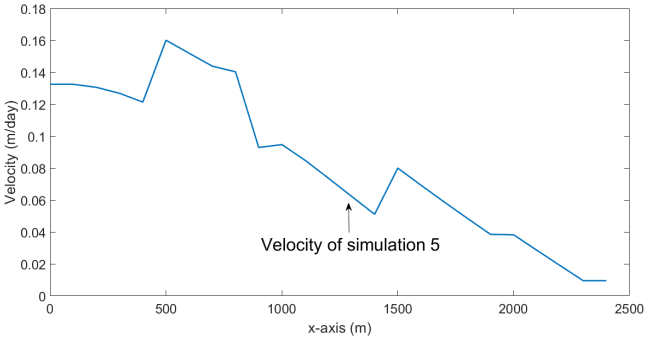

Fig. 12. The line graph of velocity in x - direction of simulation 5 at $t = 3600$ day and $y = 1200$ m

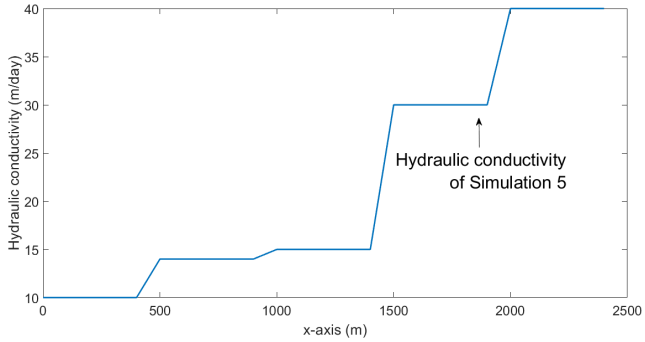

Fig. 13. The line graph of hydraulic conductivity of simulation 5 at $t = 3600$ day and $y = 1200$ m

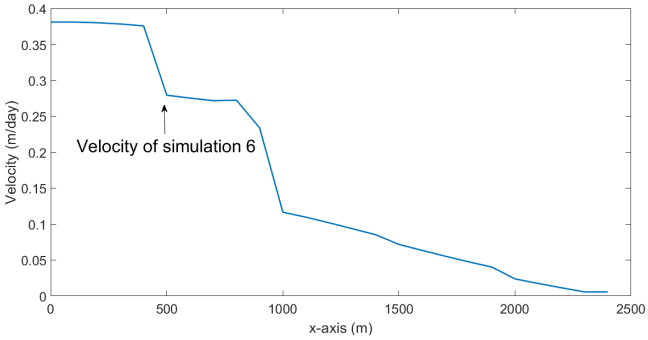

Fig. 14. The line graph of velocity in x - direction of simulation 6 at $t = 3600$ day and $y = 1200$ m

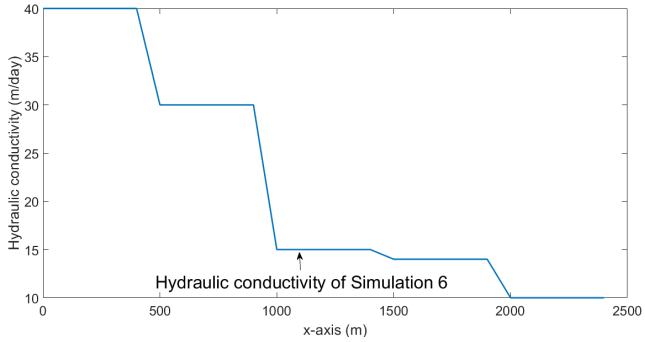

Fig. 15. The line graph of hydraulic conductivity of simulation 6 at $t = 3600$ day and $y = 1200$ m

V. Discussion

In simulation 1, we consider low level of difference hydraulic head. The results of hydraulic head, velocity flow and groundwater pollutant concentration are shown in Table I - III, respectively. The line graphs of hydraulic head, velocity in x - direction and groundwater pollutant concentration are shown Figure 1 - 3, respectively.

In simulation 2, we consider high level of difference hydraulic head. The result of hydraulic head, velocity flow and groundwater pollutant concentration are shown in Table IV - VI, respectively. The line graph of groundwater pollutant concentration is shown Figure 4.

In simulation 3, we consider low level of difference hydraulic head with five injection wells. The result of hydraulic head, velocity flow and groundwater pollutant concentration are shown in Table VII - IX, respectively. The line graph of groundwater pollutant concentration is shown Figure 5.

In simulation 4, we consider low level of difference hydraulic head with fifteen injection wells. The result of hydraulic head, velocity flow and groundwater pollutant concentration are shown in Table X - XII, respectively. The line graph of groundwater pollutant concentration is shown Figure 6.

In simulation 5, we consider low level of difference hydraulic head with five injection wells and ascending hydraulic conductivity. The result of hydraulic head, velocity flow and groundwater pollutant concentration are shown in Table XIV - XVI, respectively. The line graph of groundwater pollutant concentration is shown Figure 7.

In simulation 6, we consider low level of difference hydraulic head with five injection wells and descending hydraulic conductivity. The result of hydraulic head, velocity flow and groundwater pollutant concentration are shown in Table XVIII - XX, respectively.the line graph of groundwater pollutant concentration is shown Figure 8.

From simulations 1 - 6, the hydraulic head drives groundwater flow from the higher hydraulic head zone to the lower zone. Each area position near landfill has a higher velocity flow than faraway positions, and each area position at high velocity flow has a higher groundwater pollutant concentration than low velocity flow.

We take the velocity flow into consideration in each simulation in Simulation 7. Figure 9 demonstrates the x - direction comparison velocity flow between simulations 1 and 2. We will have a higher hydraulic head difference as well as a high velocity. Figure 10 demonstrates the x-direction comparative velocity flow between simulations 2, 3, and 4. Flow velocity is affected by the pumping of water from injection wells. There is minimal velocity in the faraway location as well. Figure 11 illustrates the x-direction comparative velocity flow for each derivative H_E. When the far area has a lower hydraulic head level, we will raise the velocity. Figure 12 - 15 illustrate the x-direction comparative velocity flow between simulations 5 and 6. When a region has a high hydraulic conductivity, the velocity of flow increases, and when the area has a low hydraulic conductivity, the velocity of flow decreases.

For all simulation, the building of landfills should be built in the area low level of difference hydraulic head. Moreover, the pumping wells around landfill can be decrease groundwater pollutant concentration before residential area. The resulted in improved water quality in the faraway area with little influence on groundwater volume and flow velocity.

VI. Conclusion

The hydraulic head drives groundwater flow from the higher hydraulic head zone to the lower hydraulic head zone in simulations 1-6. Each area position near a landfill has a higher velocity flow than those further away, and each area position with a high velocity flow has a higher groundwater pollutant concentration than those with a low velocity flow. The velocity flow is increased when the area has high hydraulic conductivity, and the velocity flow is decreased when the area has low hydraulic conductivity.

In all scenarios, landfill construction should be done in an area with a low hydraulic head. Furthermore, pumping wells near landfills might reduce the concentration of pollutants

in groundwater in residential areas. As a result, the calculated water quality in the faraway area was improved while groundwater volume and flow velocity were preserved.

REFERENCES

[1] C. W. Cryer, "On The Approximate Solution of Free Boundary Problems Using Finite Difference", *J. Assoc Comput Mach*, vol. 17, no. 3, pp397-411, 1970.

[2] J. P. Bardet and M. Tobita, "A Practical Method for Solving Free-surface Seepage Problems", *Comput Geotech*, vol. 29, pp451-475, 2002.

[3] M. T. Ayvaz, M. Tuncan, H. Karahan and A. Tuncan, "An Extended Pressure Application for Transient Seepage Problems with a Free Surface", *J. Pourous Media*, vol. 8, no. 6, pp613-625, 2005.

[4] C. S. Desai and G. C. Li, "A Resisual Flow Procedure and Application for Free Surface Flow in Porous Media", *Adv Water Resour*, vol. 6, pp27-35, 1983.

[5] N. Kikuchi, "An Analysis of The Variational Inequalities of Seepage Flow by Finite-element Methods", *Quarter Appl Math*, vol. 35, pp149-163, 1977.

[6] G. Tatfur, D. Swiatek, A. Wita and V. P. Singh, "Case Study : Finite Element Method and Artificial Neural Network Models for Flow Through Jeiorsko Earthfill Dam In Poland", *J Hydraulic Eng*, vol. 131, no. 6, pp431-440, 2005.

[7] T. N. Olsthoorn, "The Power of Electronic Worksheet : Modeling Without Special Programs", *Ground Water*, vol. 23, no. 3, pp381-390, 1985.

[8] H. Karahan and M. T. Ayvaz, "Transient Groundwater Moedeling Using Spreadsheets", *Advance in Engineer Software*, vol. 36, pp374-384, 2006.

[9] N. Pongnoo and N. Pochai, "A Numerical Computation of Non-dimensional Form of a Mathematical Model of Soil Salinity Profile in a Rice Field near Marine Shrimp Aquaculture Farm", *Adv Studies Theor Phys*, vol. 5, no. 4, pp185-191, 2011.

[10] N. Pongnoo and N. Pochai, "Numerical Tratment of a Couple Mathematical Models of Ground Water Flow in Rice Field near Marine Shrimp Aquaculture Farm", *Appl Math Sci*, vol. 6, no. 6, pp283-289, 2012.

[11] N. Pongnu and N. Pochai, "Numerical Simulation of Groundwater Measurement Using Alternating Direction Methods", *Journal of Interdisciplinary Mathematics.*, vol. 20, no. 2, pp513-541, 2017.

[12] N. Pongnu and N. Pochai, "Mathematical Simulation of Groundwater Management in a Drought Area Using an Implicit Finite Difference Method", *Thai Journal of Mathematics.*, vol. 17, no. 3, pp663-672, 2019.

[13] J. Limthanakul and N. Pochai, "A Two-dimensional Mathematical Model for Long-term Contaminated Groundwater Pollution Measurement around a Land Fill", *Mathematics and Statistics*, vol. 8, no. 1, pp61-74, 2020.

[14] S. Khatbanjong and N. Pochai, "A Long-term Numerical Groundwater Quality Assessment Model Using a Modified Fourth-order Finite Difference Method with Saulyev Scheme", *Journal of Interdisciplinary Mathematics*, vol. 23, no. 7, pp1405-1434, 2020.

[15] S. Khatbanjong and N. Pochai, "Numerical Groundwater Quality Assessment Model Using a New Fourth-order Scheme with Saulyev Method", *Journal of Interdisciplinary Mathematics*, vol. 23, no. 7, pp1287-1308, 2020.

[16] W. Timpitak and N. Pochai, "Numerical Simulations to One-dimensional Groundwater Pollution Measurement Model Through Heterogeneous Soil", *IAENG International Journal of Applied Mathematics*, vol. 50, no. 3, pp558-565, 2020.

[17] J. Limthanakul and N. Pochai, "A Mathematical Model of Horizontal Averaged Groundwater Pollution Measurement with Several Substances due to Chemical Reaction", *Mathematics and Statistics*, vol. 8, no. 6, pp645-655, 2020.

[18] S. Khatbanjong and N. Pochai, "Numerical Groundwater Quality Assessment Model Using Two-level Explicit Methods", *Engineering Letters*, vol. 29, no. 1, pp183-190, 2021.

N. Pochai is a researcher of Centre of Excellence in Mathematics, MHESI, Bangkok 10400, Thailand.

N. Pongnu is an assistant researcher of Centre of Excellence in Mathematics, MHESI, Bangkok 10400, Thailand.